Physical Science International Journal

25(1): 8-22, 2021; Article no.PSIJ.66543
ISSN: 2348-0130

Experimental Study of a Stationary Hot Air Solar Collector Built with Hemispherical Concentrators and Enhanced with Fresnel Lenses

Thierry S. M. Ky[1*], Salifou Ouedraogo[1], Moctar Ousmane[1,2], Boureima Dianda[1,3], Emmanuel Ouedraogo[1,4] and Dieudonné J. Bathiebo[1]

[1]Laboratory L.E.T.RE, University Joseph KI-ZERBO, Ouagadougou 03 PO Box 7021, Burkina Faso.
[2]University of Agadez, PO Box 199, Niger.
[3]IRSAT, Ouagadougou 03 PO Box 7047, Burkina Faso.
[4]Department of Physics and Chemistry, University of Ouahigouya, Burkina Faso.

Authors' contributions

This work was carried out in collaboration among all authors. Author TSMKy' designed the study, performed the statistical analysis, wrote the protocol, and wrote the first draft of the manuscript. Authors SO and MO managed the analyses of the study. Authors BD and EO managed the literature searches. All authors read and approved the final manuscript.

Article Information

DOI: 10.9734/PSIJ/2021/v25i130233
Editor(s):
(1) Professor. Pratima Parashar Pandey, Dr. APJ Abdul Kalam Technical University, India.
(2) Dr. Thomas F. George, University of Missouri–St. Louis (UMSL), USA.
Reviewers:
(1) Razika Ihaddadene, Mohamed Boudiaf University of M'sila, Algeria.
(2) Simo-Tagne Merlin, University of Larraine, France.
Complete Peer review History: http://www.sdiarticle4.com/review-history/66543

Original Research Article

Received 07 December 2020
Accepted 12 February 2021
Published 17 February 2021

ABSTRACT

Aims: This paper is about a solar collector made of hemispherical concentrators. This collector is sun tracking free, and used for natural convection. Lenses are used on top of each concentrator to improve its efficiency.
Study Design: The Solar collector is made of hemispherical concentrators with Fresnel lenses axially-centered to those concentrators and placed on top of each one of them. Those concentrators are covered with a 4 mm glass for a greenhouse effect. The concentrators generate hot spots that heat the inside air. There is no need for receivers at the hot spots.
Methodology: from Inlet to outlet, temperatures are measured as well as inlet air speed, which allow the efficiency evaluation.
Results: Although those measurements were conducted in a cloudy period, temperature difference

**Corresponding author: E-mail: thierrysmky@gmail.com;*

from the inlet to the outlet was around 55°C to 65°C. This result is superior to previous studies of the same system without lenses which gave temperature difference around 35°C to 45°C. It is sharply superior to that of usual black-painted convective system with fined plates that gives a temperature difference of around 20°C to 25°C.

Conclusion and Perspectives: The global efficiency calculated using measurement values reaches 56%. This is far greater compared to previous black plate systems' efficiency of 29%, giving an efficiency increase of 93%, but expected knowing that we are using a concentration system for convection.

Keywords: Solar bowl; spherical concentrator; natural convection; hot air solar collector; efficiency and fresnel lenses; stationary tracking free permanent system.

1. INTRODUCTION

Solar collectors for fluids heat-up never stop evolving. Most of them use an absorber which is a black-painted plate or black plastic tubes to collect solar heat by fluid circulation and through natural or forced convection. This type of collectors had been intensively studied. Their common use is for swimming pool water heat if their fluid is liquid [1], or solar dryers if their fluid is air [2]. When these collectors are put under a transparent glazing such as plastic or glass, their heating capacity increases due to the additional greenhouse effect [3]. Solar chimneys [4], Cirrillo et al., [5], Al-Kayiem and Aja, [6] and dryers [7], Arunsandeepa et al., [8], Simo-Tagne et al., [9-11]) are using this technology as collector with more or less variants. All those collectors which can be permanently fixed, meanwhile with no sun-tracking engine [12], barely bring temperature variation around 20°C to 25°C from the inlet to the outlet. To go higher, arriving sun lights need to be concentrated 2003 [13] and the collector needs a sun-tracking mechanism [14].

These times, a novel type of solar collectors using hemispherical concentrators has been investigated [15]. These hemispherical concentrators had been used due to the fact that while also being permanently fixed, sun-tracking free, they still concentrate solar rays [16], El-Refaie, [17], Gandhe et al, [16,18], Kreider, [19], Steward and Kreith, [20], Ky et al., [21]. Therefore, using them to build stationary collectors was possible [22], gaining additional temperature increase in accordance with the hot spot theory [23]. The functioning principle relies mainly on the geometry of the solar bowl, which does not change with the hour and declination angles [22]. Also, there is no need to place a receiver or absorber at the focal point, the air inside is heated through convection and greenhouse effects [24]. Some solar hot air dryers were built using these collectors with the guaranty of drying products needing even higher temperatures up to 65 – 80°C [22]. These collectors had been also proposed to enhance air pushing (or pulling) systems such as solar chimneys [24].

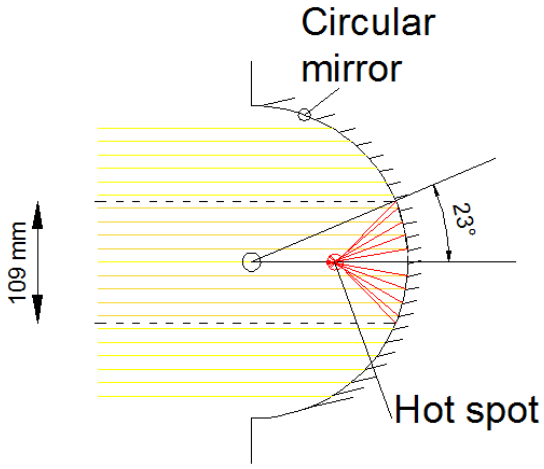

Fig. 1. Concentration on a circular mirror of parallel rays. The Aperture area contributing to the Hot spot is defined by the half angle = 23° which corresponds to 0.39 time the radius of the circle

However, the arriving sunrays being parallel, for an area equal to the surface made by the radius of the sphere, only 0.15 time the aperture area contribute to this hot spot [23], as shown by Fig. 1.

Beyond the 23° half angle value, the sun image moves from a dot shape "hot spot" to a conical shape [21], and the concentration effect on air is sharply reduced. The rays colored in yellow do not contribute to the hot spot, delimited by the dashed lines. The orange-colored ones are those whose contribute to the hot spot. This contribution does not change with the rays arriving with an angle unless shadowed by the bowl's wall.

In this paper, we are proposing to build a collector with hemispherical concentrators and to place on top of each concentrator, a Fresnel lens. We will therefore make measurements to evaluate the temperatures along the system and calculate the efficiency of the new collector.

2. MATERIALS AND METHODS

Rays coming from a lens to a circular concentrator also get concentrated the same way like rays coming to a hemispherical concentrator from a spherical diopter as previously studied [25]. We therefore get a double concentration that increases the aperture area contribution to the hot spot.

2.1 Theoretical and Optical Analysis of the System

The proposed system is built with a hemispherical concentrator (or solar bowl) using solar rays concentrated by a lens or Fresnel lens, or a ring array concentrator – RAC [26], Mouzouris et al. [27]. The lens is disposed axially-centered with the solar bowl. The parallel sunrays arrive on the lens and are concentrated with a certain focal distance quite greater than the distance between the lens and the concentrator's bottom. The concentrated rays arriving from the lens are re-concentrated to the hot spot by the bowl. With this system, a greater part, if not all of the lens surface, meaning a wider part of the aperture area is contributing to the hot spot and supposedly bringing more convection effect to the air flow, as shown on Fig. 2.

For instance, for a lens 240 mm of diameter and a hemispherical concentrator 280 mm of diameter, with a gap of 50 mm between the lens and the bowl, the ratio of the aperture area which contributes to the hot spot is equal to 0.74.

Somehow, the Fig. 2 is about sunrays coming perpendicularly to the lens' surface. We should analyze the system with sunrays coming with an angle. Based on previous study of a lens concentrating on a target with rays arriving on the lens with a certain acceptance angle [28], we will study graphically the part that concentrates to the hot spot as shown on Fig. 3.

By using the color code, we see that the aperture area contributing to the hot spot is kept for rays coming on the lens with acceptance angles slightly superior to 15°, but starts getting reduced with angle. In our case for instance where we made representation for angles up to 45°, we have a ratio of 0.26 of aperture area (after multiplication to the rays' angle cosine), that contributes to the hot spot. This reduction of aperture area contribution is due to the lens coma: the yellow rays are indeed convergent, but the convergence is appearing too soon so at the hemispherical reflective surface, they become divergent.

However, the aperture area's ratio of 0.26 for sunrays arriving on the lens with an acceptance angle of 45°, which represents an angle corresponding to 9h00 in the morning or 15h00 in the afternoon, is still higher than that of the previous system without lens which is only 0.15 at all time. This suggests that the system can be used from 9h00 to 15h00 without sun-tracking system and we postulate to obtaining better result than the previous system.

We also see an eccentricity of the hot spot of 0 to d3 from the axis of symmetry (Fig. 3) with the increase of the acceptance angle, but that will not be of any prejudice since there is no disposal of target at the hot spot.

The collector efficiency η in % can be evaluated using the following formula.

$$\eta = 100 \frac{\sum_{n} q_m C_p (T_{out} - T_{in})}{I_r(t, \varpi) S} \quad (1)$$

With:

q_m the air mass flow rate in kg.s^{-1}

C_p =1006 J.kg^{-1}.K^{-1}, the specific heat capacity of the air.
T_{out} the temperature of air outing the collector in K
T_{in} the temperature of air entering the collector in K
$I_r(t,\varpi)$ the solar radiation at the measured time and radiation angle cosine due to time in W.m^{-2}
S the collector exposed section to the sun in m^2

The following relation will be used to evaluate the air mass flow :

$$q_m = \rho_i v_i s_i \quad (2)$$

With:

ρ_i the air density at the i flow section in kg.m^{-3}
v_i the air velocity at the i flow section in m.s^{-1}
s_i the section size at i in m^2

The density variation with the temperature will be estimated by the following relation, considering the air being a perfect gas:

$$\rho_i = 1.292 \frac{T_0}{T_{in}} \quad (3)$$

With:

T_0 =273.15K.

The air flow section for measurement was taken at the entry of the collector, and the temperature used for velocity calculation is of the ambient air.

2.2 Conception of the Prototype

The prototype of the collector is composed of 3 bowls encased in an insulated box. The insulation is made by 4 mm polyester entirely covering the inner surface of the box. These bowls are covered with a glazing 4 mm thick and 45 mm distant to the edge of the bowls. A Fresnel lens is axis-symmetrically positioned over each bowl. The overall collector is positioned 12° angle with the horizontal, which is equal to the latitude angle of Ouagadougou (Burkina Faso) and the slop is towards the North to obtain an annually stationary (sun-tracking free) positioning, as noted in Fig. 4.

The lenses used for our prototype are Fresnel lenses having the following characteristics:

- Circular Fresnel lenses. Diameter=240 mm, focal distance=260 mm.

The following table (Table 1) shows the quote part of the aperture area that contributes to the hot spot according to the aperture angle ϕs, the solar rays coming angle on the system and the zone of the lenses that is not submitted to comas. That zone varies according to the rays' angle: It is considered full from 0 to 15°, half at 30° and 44% at 45°.

As we can see on the table, the problem with the use of lenses is that the aperture area shall be multiplied by the cosine of the rays' angle to define the area contributing to the hot spot. Nevertheless, this area is greater than that of the former studies without lenses between 9 am. to 3 pm.

The solar bowls in our system are a reuse of IKEA's BLANDA BLANK salad mixing bowls 280 mm of diameter. These bowls are made of stainless steel and have a chromed reflective inner surface. The Fresnel lens is placed on top of the cover glass 4 mm thick, axially-centered with the bowls and the gap between the glass and the bowls is 45 mm. The Lenses have also a 5 mm gap with the glass, knowing that those lenses will not stand temperatures above 80°C.

2.3 Functioning Principle of the System

The sunrays coming on each Fresnel lens is concentrated into the corresponding hemispherical concentrator to generate a hot spot. The air coming from the inlet will get charged with heat till the outlet where it gets sufficient kinetic energy and heat, moving by thermosyphon as noted in Fig. 5.

The system is just like hot spot theory systems previously studied [29], except that the part of the aperture area contributing to the hot spot is substantially increased by Fresnel lenses. Meanwhile, in order to furtherly increase the outlet temperature, all the previous proposed ameliorations such as the division of the hot spot domain into bands to reduce the volume of air for better heat up [25] and the truncating of the bowls to keep the useful parts regarding the declination angle [22] stand as well for our new system.

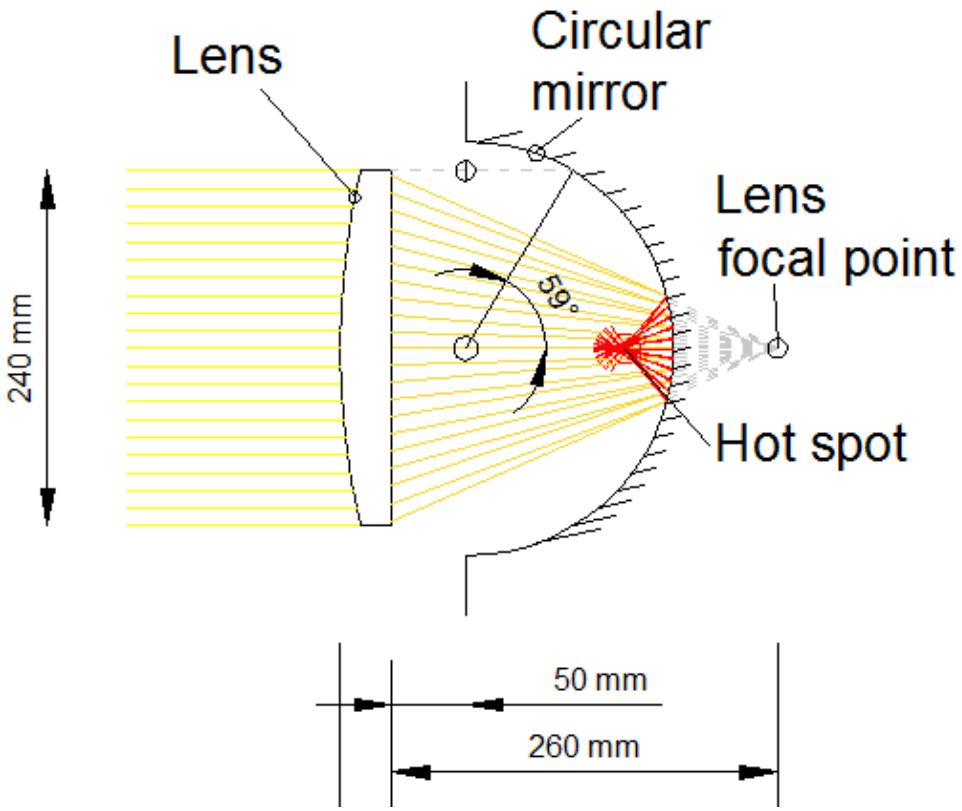

Fig. 2. Concentration in a circular mirror through a lens. The aperture area contributing to the Hot spot is defined by the half angle = 59° which corresponds to 0.86 time the radius of the bowl and the radius of the lens

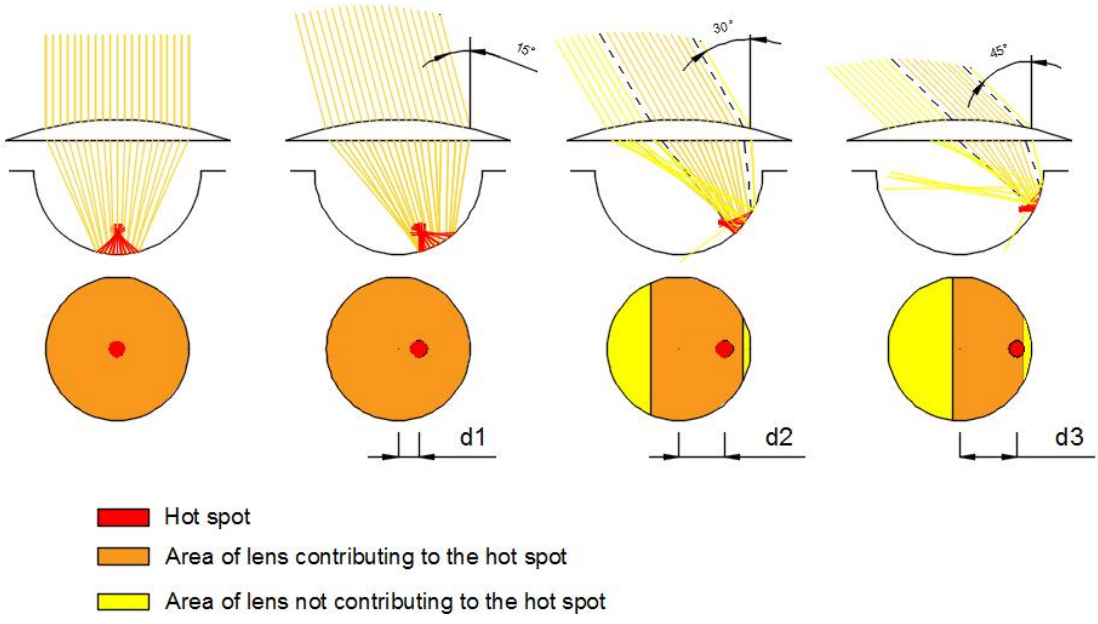

Fig. 3. Influence of arriving sunrays' acceptance angle on the lens

Fig. 4. Photo of the system

Table 1. Ratio of aperture area contributing to the hot spot according to the lens diameter and the arriving solar rays' angle

Lenses	ϕ_s	Radius portion Contributing to the hot spot	Solar rays' angle α = 0°	Solar rays' angle α = 15°	Solar rays' angle α = 30°	Solar rays' angle α = 45°
Without	23°	$0.39R_s$	0.15	0.15	0.15	0.15
D=240 mm	59°	$0.86R_s$	0.74	0.71	0.37	0.26

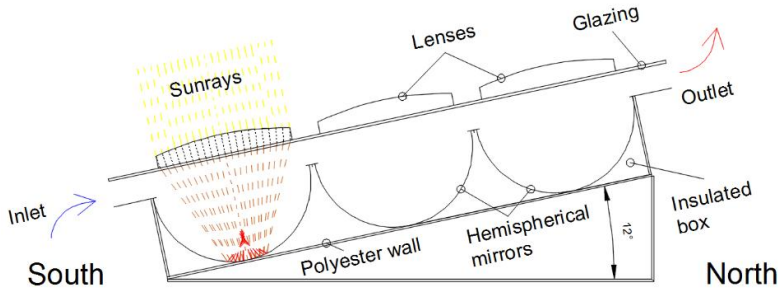

Fig. 5. Schema of the collector

To study the system experimentally, we used the following equipment and measurement methodology:

- A data logger Midi LOGGER GL220A of GRAPHTEC brand.
- A probe Amb for ambient temperature measurement
- Probes (Thermocouples) Tb1 to Tb3 for measurement of temperatures at bowls junctions as indicated on Fig. 6. The probes do not touch the metallic part of the bowls.
- Probes Th1 to Th3 for measurement of temperatures over each corresponding Tb probes and under the glass coverage. This way, we can get the temperatures outing each bowl by obtaining a mean temperature of the upper and lower probes.
- A pyranometer SR03-05 of Hukseflux brand to measure global insolation. Its sensibility is 7.64 µV ($W.m^{-2}$). Its accuracy (or uncertainty) will be considered as follow: Second class material used in summer mid-latitude = 8.4%
- A hot wire anemometer Model YK-2004AH with ± (5% of reading + $0.3km.h^{-1}$) of accuracy.

K type thermocouples were placed to evaluate the temperature increase along the way to the outlet. The ones placed down (Tb_i) are not touching any metallic part but the air, as well as the ones placed under the glass (Th_i) which are not touching it, as indicated on Fig. 6. Their accuracy for temperatures measurements with the data logger are: -100°C< Temp. <1370°C ± (0.05% of reading + 1.0°C).

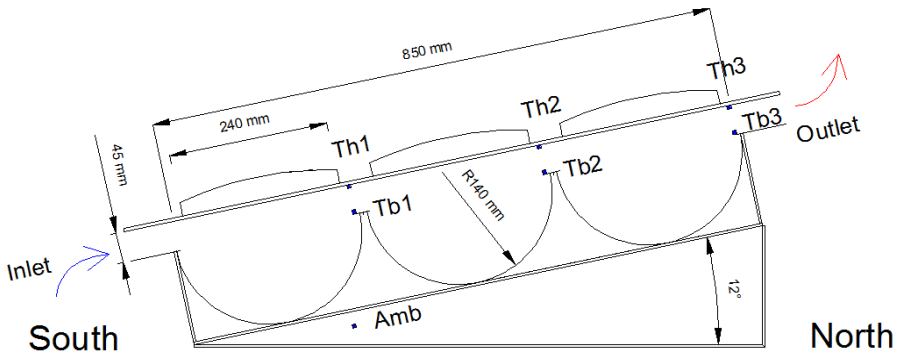

Fig. 6. Probes position for temperature measurement

Probe Amb. is placed on a shadow around one meter over the floor.

The prototype useful dimensions are 1000 mm long per 300 mm width, corresponding to the exposition area of the collector. Air circulation inlet and outlet sections are 300 mm width per 45 mm height. The three bowls 280 mm of diameter are aligned.

The prototype is fixed steadily during the measuring process, it is oriented with the slot towards the north and leaned 13° which is the angle corresponding to the latitude of Ouagadougou.

Filters are placed at the inlet and outlet to avoid dust admission.

There is no need to track the sun, keeping the advantages of usual collectors.

The temperature and insolation probes' measurement results of the day are collected directly by the data logger any 5 minutes, and the files are treated first with EXCEL and curves drawn by MATLAB software.

3. RESULTS AND DISCUSSION

Measurements were taken between September 28th and September 30th, 2019. We hardly passed the equinoxe which was at September 23rd, but in Burkina Faso, we are just getting out of the rainning season, with lots of clouds in the sky. This may reduce the direct sunrays coming on the collector.

Additonal measurement was made in March 13th, 2020, including air speed readings to evaluate the efficiency. That period is one of the worst due to the atmosphere being charged with fine particules coming from the Sahara desert and masking the sun. Direct sunlight may be consequently reduced.

3.1 Measurement of September 28th, 2019

Measurement of insolation was taken on September 28th, 2019 and the following curve shows its evolution with time (Fig. 7). We can see how some cloud coverage interacted with the arriving direct sunlight. The peak value was around 940 W. m^{-2}.

Temperature measurements (Fig. 8) show all the curves having the same shape as the one of the insolation, with imperfections in accordance with the cloud coverages. We added error bars only at the outlet temperature curves and the ambient temperature curve.

Heat progression is also noticeable with temperatures of last probes (Th3, Tb3) being higher than those of the firsts. The pic reached 103°C with probe Tb3. Temperature of those probes evolved above 60°C from 9:00 am to 4:00 pm.

3.2 Measurement of September 29th, 2019

Measurement of insolation was taken on September 29th; 2019 (Fig. 9). The afternoon was quite disturbed by cloud coverages. The peak value was whatsoever around 920 W.m^{-2}.

Temperature measurements (Fig. 10) show all the curves normally evolving in the morning, but from 12:20 pm, we observe a sharp decrease due to cloud coverages. We added error bars only at the outlet and the ambient temperature curves.

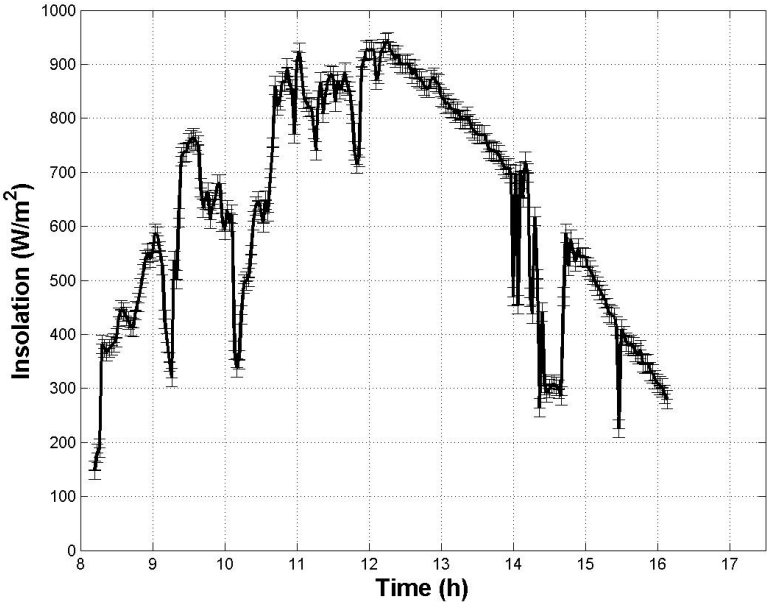

Fig. 7. Solar radiation evolution as a function of time for september 28th, 2019. Measurement from 8:10 am to 4:10 pm

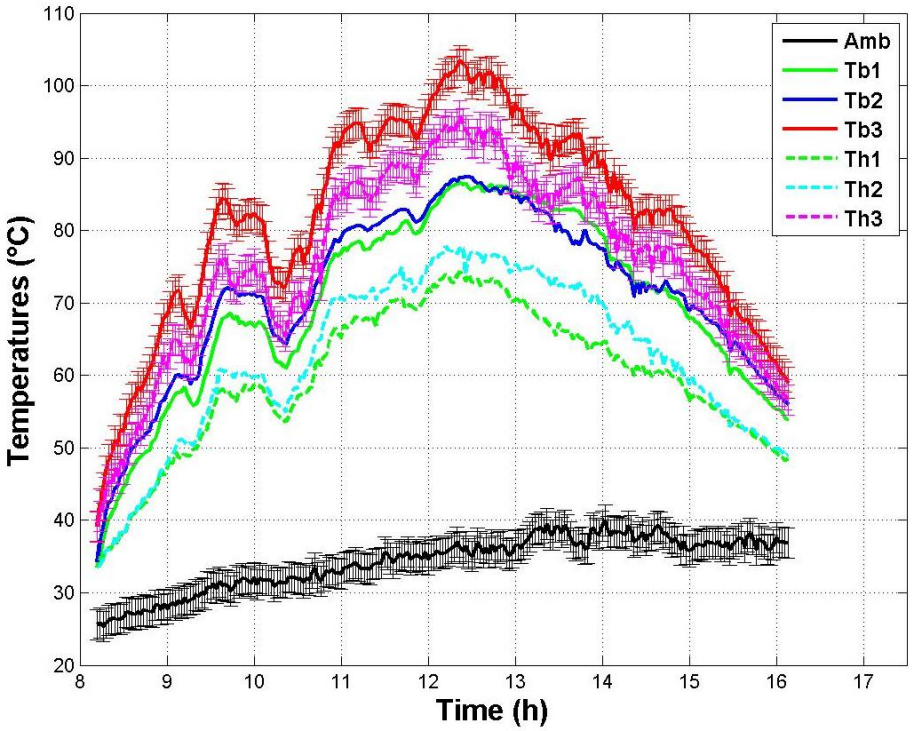

Fig. 8. Temperature measurements evolution as a function of time for September 28th, 2019 from 8:12 am to 4:10 pm

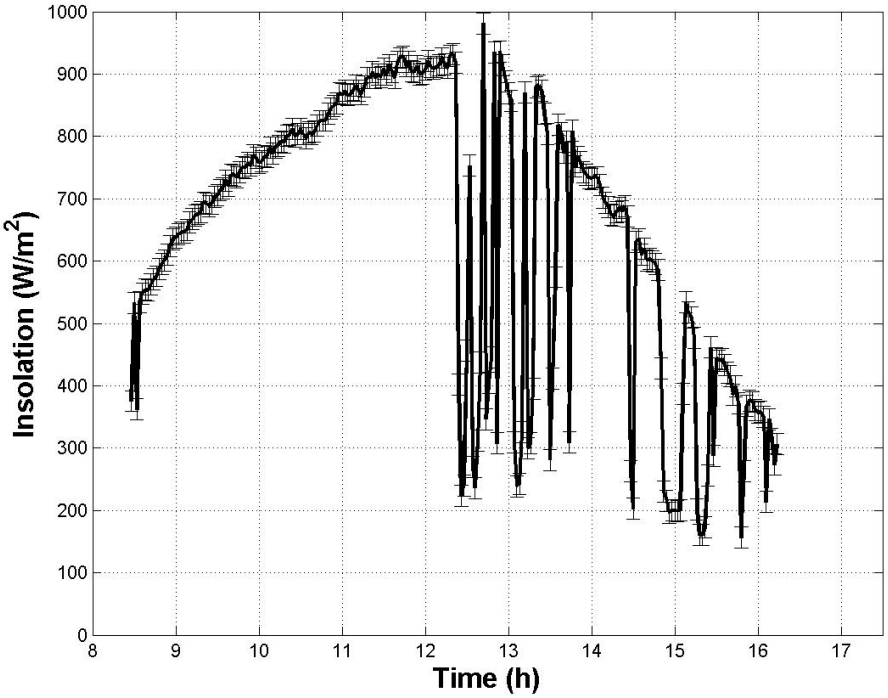

Fig. 9. Solar radiation evolution as a function of time for september 29th, 2019. Measurement from 8:30 am to 4:10 pm

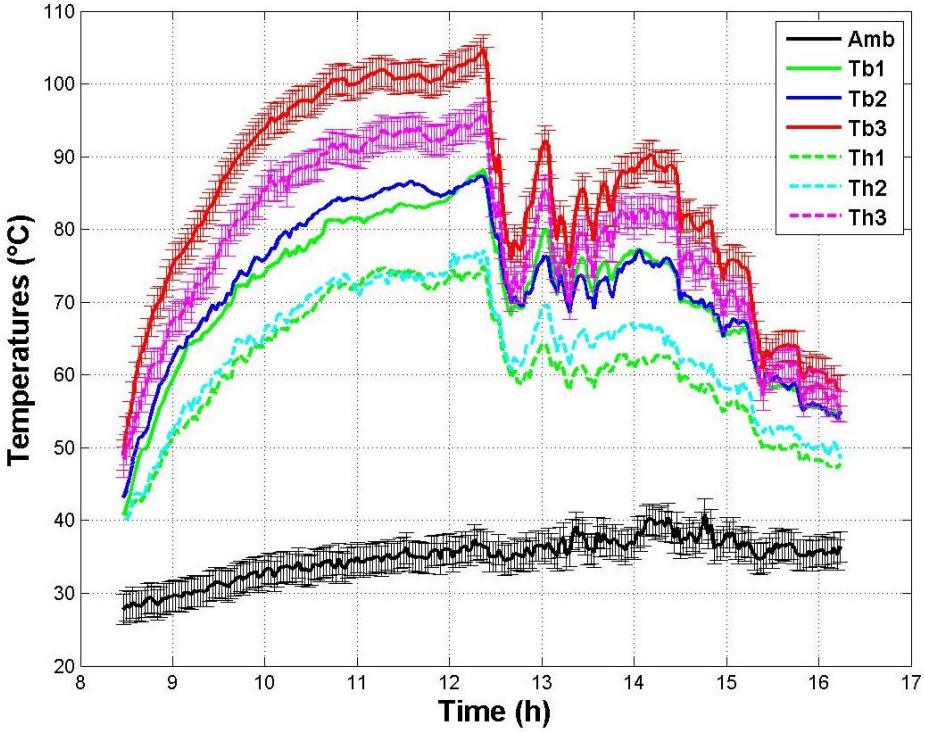

Fig. 10. Temperature measurements evolution as a function of time for September 29th, 2019 from 8:25 am to 4:10 pm

Last probes (Th3, Tb3) have higher temperature than the firsts, showing evolution of temperatures with natural convection phenomenon. The pic reached 105°C with probe Tb3. Temperature of those probes evolved above 60°C from 9:00 am to 4:00 pm, even with all the perturbations of the afternoon.

3.3 Measurement of September 30th, 2019

Measurement of insolation was taken on September 30th (Fig. 11). The afternoon was barely disturbed by cloud coverages, which happened around 1:30 pm and 2:40 pm. The peak value was around 920 $W.m^{-2}$.

Temperature measurements (Fig. 12) show all the curves with normal shapes throughout the day, with some disturbances in the afternoon in accordance with the cloud passages.

Last probes (Th3, Tb3) have higher temperature than the firsts as previously noticed. The pic reached 97°C with probe Tb3. Temperature of those probes evolved above 60°C from 9:00 am to 4:00 pm.

3.4 Measurement of March 13th, 2020

Additional Measurement of insolation was taken on March 13th (Fig. 13) to evaluate the efficiency of the system. The shape of the curve is perfect, except that the atmosphere was charges with tiny particles, shadowing the sun. The peak value was around 800 $W.m^{-2}$.

Temperature measurements (Fig. 14) show all the curves with normal shapes throughout the day. We added error bars only at the outlet temperature curves and the ambient temperature curve.

Last probes (Th3, Tb3) have higher temperature than previous ones. The pic reached 91°C with probe Tb3. Temperature of those probes evolved above 50°C from 9:00 am to 4:00 pm. We notice somehow a weak global decrease of the temperatures due to the sun coverage with dust particles.

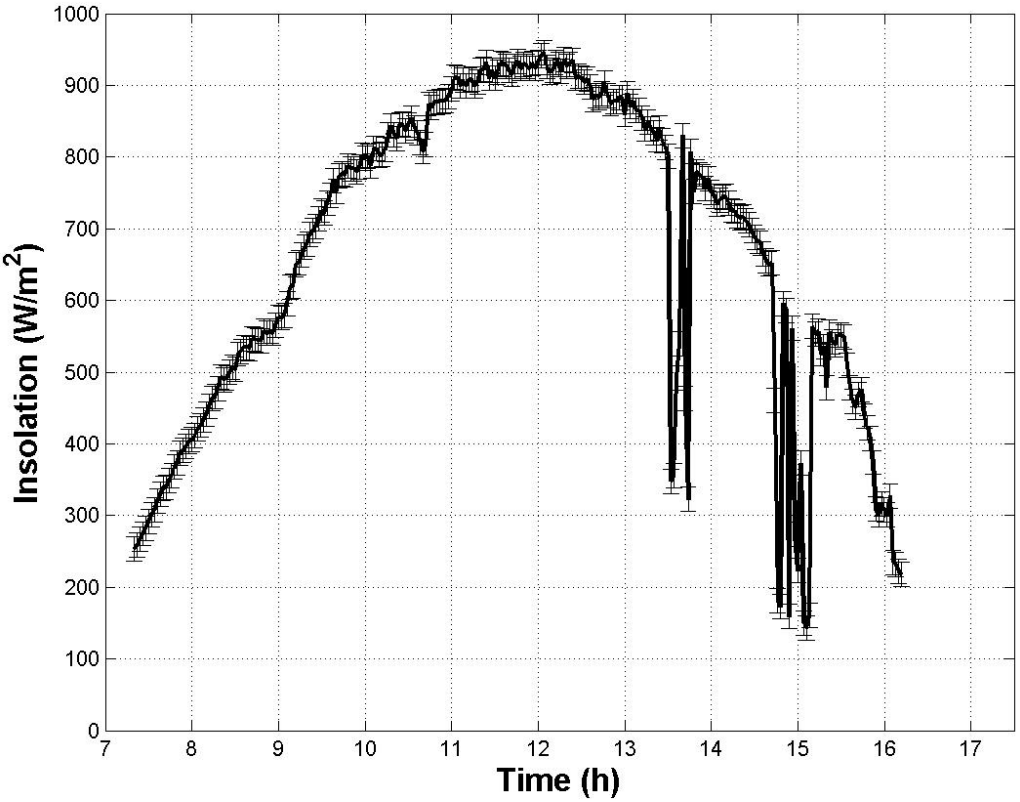

Fig. 11. ***Solar radiation evolution as a function of time for*** **September 30th, 2019. Measurement from 7:20 am to 4:10 pm**

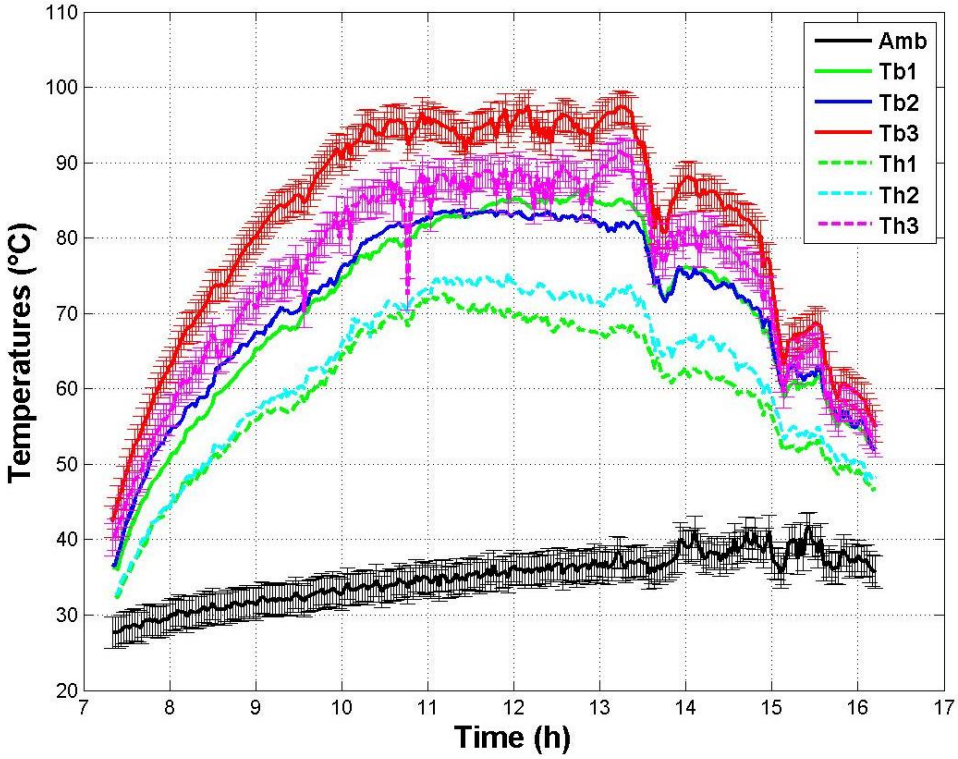

Fig. 12. Temperature measurements evolution as a function of time for September 30th, 2019 from 7:20 am to 4:10 pm

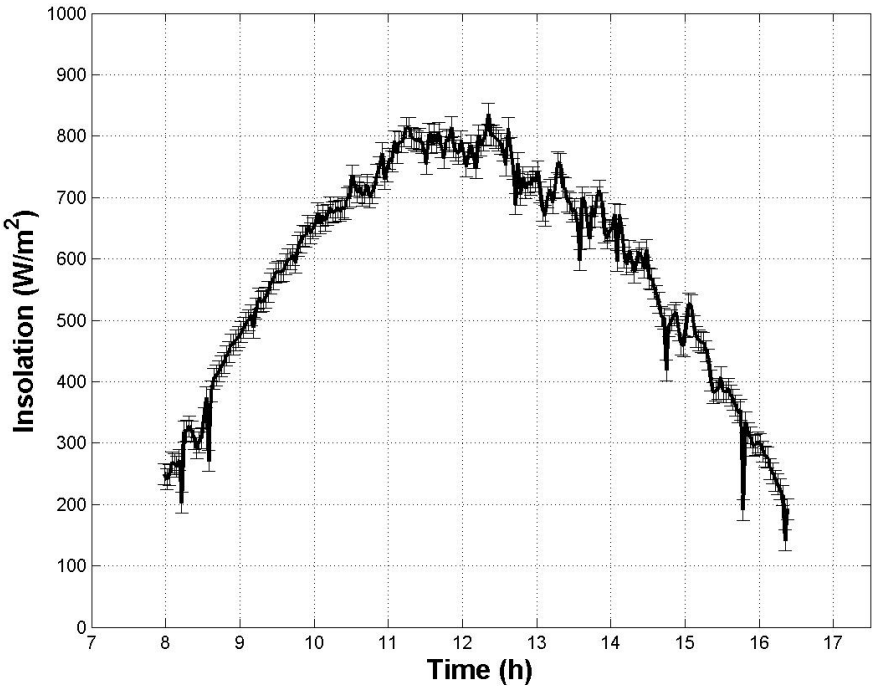

Fig. 13. Solar radiation evolution as a function of time for March 13th, 2020. Measurement from 8:00 am to 4:20 pm

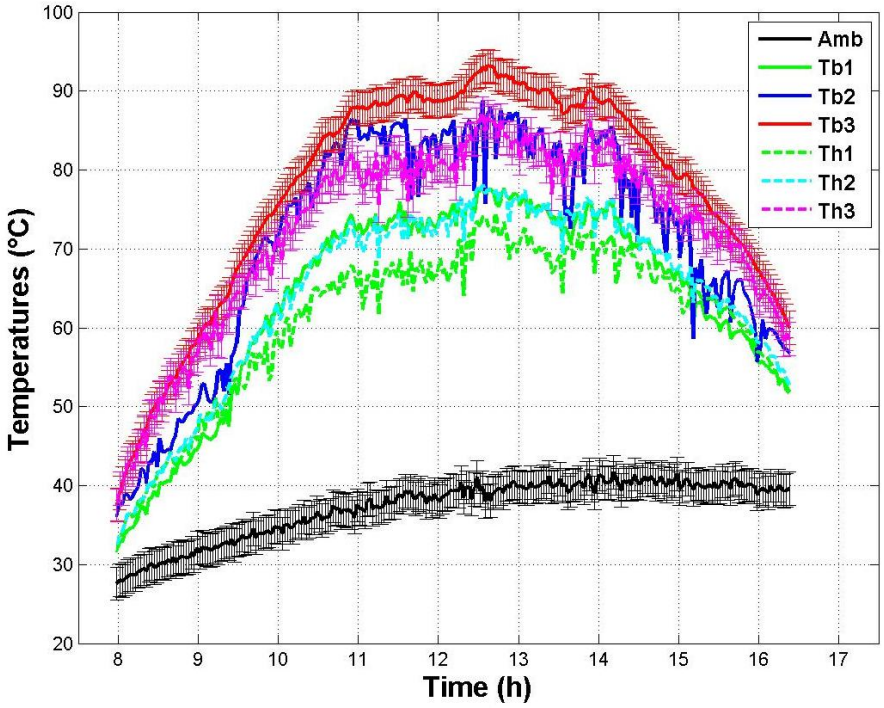

Fig. 14. Temperature measurements evolution as a function of time for March 13th, 2020 from 8:00 am to 4:20 pm

The following Fig. 15 show the inlet air speed taken at the 60 mm inlet diameter, and the efficiency. The anemometer is less sophisticated, so we had to take the speed measurement each 30 mn, and evaluate the efficiency using the other temperature and Insolation readings corresponding to the time of speed reading.

The air speed evolves from 1.8 $km.h^{-1}$ at 11:00 am to 3.5 $km.h^{-1}$ at 01:00 pm. It then decreases to 1.1 $km.h^{-1}$ at 15:45 pm. The speed looks slow due to the only 13° slop of the collector.

The efficiency was also evaluated, starting from 35% at 11:00 am to 71% at 01:00 pm. These values are higher compared to regular collectors, but are not unexpected as we are dealing with concentration. Then the efficiency drops to 51% at 03:45 pm. The global efficiency using equation (01) is 56%.

Two notifications have to be mentioned:

1- The first concentration from the lenses brings a surface of around 90 to 100 mm of diameter on the hemispherical concentrators. This surface circles the flat bottom of the bowl 60 mm of diameter at noon, making it very prejudicial, and consequently impacting the results.

2- The 90 to 100 mm of diameter surface resulting from the lenses' concentration has a very noticeable contour that shows colors segregation like rainbows from violet at the inner side, to red at the outer side of the circle, suggesting that the sunrays coming from the lens could bring an enlargement of the hot spot diameter as well as the reflection on the bowl.

In any case, those phenomena should be evaluated.

3.5 Cost Evaluation for a Square Meter Collector

The following Table 2 gives the cost of the prototype and a cost projection for a square meter collector. Prices are given in USD, using a conversion rate of 1 USD = 0.91 Euros, to which the currency of Burkina Faso is linked.

From the measurement results, we can see an increase of temperature from previous systems without lenses to the present system. The increase is directly due to the widening of the exposition area that contributes to the hot spot.

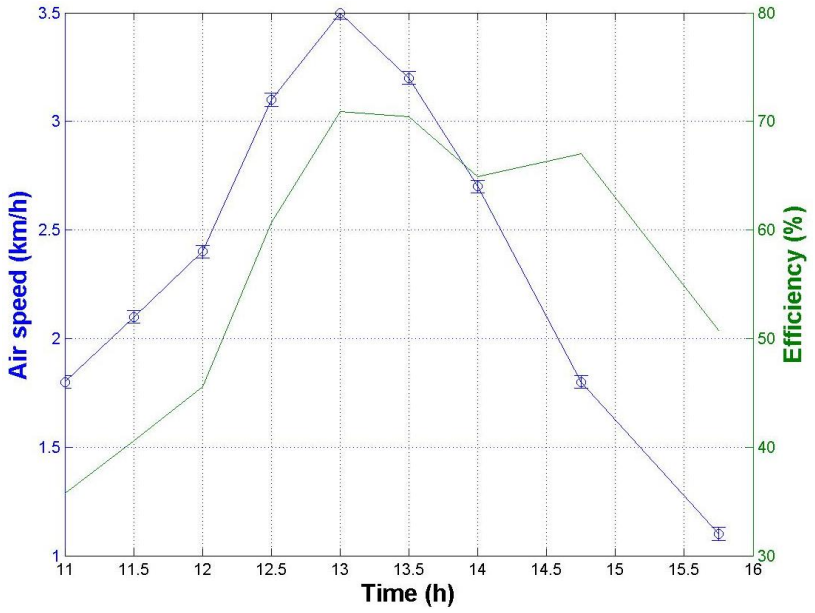

Fig. 15. Inlet air speed partial reading and efficiency evaluation in March 13th, 2020 from 11:00 am to 3.45 pm

Table 2. Realization cost of the prototype and evaluation of a square meter collector

Part	Cost of prototype	Cost projection for a square meter collector
Hemispherical bowls	27	81
Collector enclosure	67	167
Insulator material	10	20
Glass 4 mm thick	2.5	7.5
Fresnel lenses	53	160
Construction and installation	90	150
Total cost (in USD)	249.5	585.5

Even though the measurements are done in a period when the sky is cloudy or charged with dust particles, results obtained are upholding the hot spot theory, making the natural convection systems built with hemispherical concentrators, with or without lenses, better convective systems than ordinary convective ones with black-painted and fined plates, while keeping the key advantage of being stationary tracking free systems.

Ordinary results of natural convection give peak temperature difference from inlet to outlet barely superior to 25°C, while in this system, we are getting 35°C to 45°C without lenses, and 55°C to 65°C for the system with lenses.

The efficiency of 56% is far more superior to the regular efficiency, usually admitted to be around 29% (for a collector alone made of dark plate).

The overall price of a square meter collector is quite expensive, because some parts such as the hemispherical bowls and the Fresnel lenses are ordered through the internet. An industrial production could therefore reduce the price consequently.

4. CONCLUSION AND PERSPECTIVES

Results obtained after measurement the collector support the idea that the system is efficient. Its global efficiency had been evaluated and found equal to 56%. Temperature differences from inlet to outlet had increased up to 65°C in comparison with the same system without lenses, and even more compared to black-painted fined plate natural convective systems. These results are obtained in a period of partial coverage of the sky with clouds and dust particles.

As perspectives, we may investigate the actual usefulness of such convective collectors, as their use for indirect solar dryers, to solar chimney power plants and solar air pushing or pulling systems for house venting. We also consider now the building of the concentrators using local materials for social use.

ACKNOWLEDGEMENTS

The authors gratefully acknowledge the Ministry of Industry, Trade and Handicrafts of Burkina Faso (MICA-Burkina) for having supported the patent OAPI N°16893 filled by Ky and Bathiebo related to this system.

They also gratefully acknowledge the International Science Program (ISP) for supporting BUF01 and the Family Federation for World Peace and Unification Headquarter (FFWPU-HQ, South Korea) for the resources disposal to accomplish this work.

COMPETING INTERESTS

Authors have declared that no competing interests exist.

REFERENCES

1. Matteo Dongellini, Stefania Falcionia, Andrea Martellia and Gian Luca Morinia. Dynamic simulation of outdoor swimming pool solar heating. Energy Procedia. 2015;81:1–10.
2. Kabir MH, D'Souza PM, Ahsan J, Student PG. Prospects of solar energy drying technologies: A critical review. International Journal of Innovative Research in Science, Engineering and Technology. 2016;10:17866-17870. Available:http://doi.org/10.15680/IJIRSET.2016.0510081
3. Chauhan PS, Kumar A. Performance analysis of greenhouse dryer by using insulated north-wall under natural convection mode. Energy Reports 2016.2, 107–116. Available:https://doi.org/10.1016/j.egyr.2016.05.004
4. Bansod PJ, Thakre SB, Wankhade NA. Solar chimney power plant - A review. International Journal of Modern Engineering Research. 2014;4(11):18-34
5. Cirillo L, Ronza D, Fardella V, Manca O, Nardini S. Numerical and experimental investigations on a solar chimney integrated in a building facade. International Journal of Heat and Technology. 2015;33:246–254. Available:https://doi.org/10.18280/ijht.330433
6. Al-Kayiem HH, Aja OC. Historic and recent progress in solar chimney power plant enhancing technologies. Renewable and Sustainable Energy Reviews. 2016;58:1269–1292. Available:https://doi.org/10.1016/j.rser.2015.12.331
7. Bassey EMW, Schmidt OG. Solar Drying in Africa 18; 1987.
8. Arunsandeepa G, Lingayata A, Chandramohan VP, Rajua VRK, Srinivas Reddyb K. A numerical model for drying of spherical object in an indirect type solar dryer and estimating the drying time at different moisture level and air temperature. International Journal of Green Energy. 2018;1–12.
9. Simo-Tagne M, Zoulalian A, Remond R, Rogaume Y. 'Mathematical modelling and numerical simulation of a simple solar dryer for tropical wood using a collector, Applied Thermal Engineering (Elsevier). 2018;131:356-369.
10. Simo-Tagne M, Bennamoun L. Numerical study of timber solar drying with application to different geographical and climatic conditions in Central Africa, Solar Energy (Elsevier). 2018;170:454-469.
11. Simo-Tagne M, Bonoma B, Bennamoun L, Monkam L, Léonard A, Zoulalian A, Rogaume Y. Modeling of coupled heat and mass transfer during drying of ebony wood using indirect natural convection solar dryer. 2019. Drying Technology (TaylorFrancis). 2019 ;1-17. Available:https://doi.org/10.1080/07373937.2018.1544144
12. Kumar M, Sansaniwal SK, Khatak P. Progress in solar dryers for drying various commodities. Renewable and Sustainable Energy Reviews. 2016;55:346–360. Available:https://doi.org/10.1016/j.rser.2015.10.158
13. Schwarzer K, Vieira Da Silva ME. Solar cooking system with or without heat storage for families and institutions. Solar Energy. 2003;75:35–41.
14. Muthusivagami RM, Velraj R, Sethumadhavan R. Solar cookers with and without thermal storage - a review. Renewable and Sustainable Energy Review. 2010;14:691–701.

15. Thierry SM Ky, Sie Kam, Boureima Dianda, Dieudonne J Bathiebo. Optical analysis of a hemispheric concentrator with a manual tracking system for the declination. Global Journal of Pure and Applied Sciences. 2015;2:146-154.
16. Cohen S, Grossman G. Development of a solar collector with a stationary spherical reflector/tracking absorber for industrial process heat. Solar Energy. 2016;128:31–40.
Available:https://doi.org/10.1016/j.solener.2015.05.036
17. El-Refaie MF. Performance analysis of the stationary-reflector/tracking-absorber solar collector. Applied Energy 1987;28:163–189.
18. Gandhe VB, Venkatesh A, Sriramulu V. Thermal analysis of an FMDF solar concentrator. Solar and Wind Technology. 1989;3:197–202.
19. Kreider JF. Thermal performance analysis of the stationary reflector/tracking absorber (SRTA) solar concentrator. Journal of Heat Transfer. 1975;97:451.
Available:https://Doi.Org/10.1115/1.3450397
20. Steward WG, Kreith F. Stationary concentrating reflector cum tracking absorber solar energy collector: Optical design characteristics. Applied Optics. 1975;14:1509.
Available:https://doi.org/10.1364/AO.14.001509
21. Thierry SM Ky, Boureima Dianda, Moctar Ousmane, Bienvenue M Pakouzou, Sie Kam, Dieudonne J Bathiebo. Optical and thermal performance analysis of a steady spherical collector with a crescent-shaped rotating absorber. International Journal of Advanced Engineering Research and Science. 2017;4(4):234-245.
22. Thierry S Maurice Ky, Boureima Dianda, Emmanuel Ouedraogo, Salifou Ouedraogo, Dieudonné J Bathiebo. Novel Natural Convection Process: Indirect Solar Dryer Built with Spherical concentrators. Application to Tomato Drying. Elixir Thermal engg. 2018;122:51615-51620.
23. Thierry S Maurice Ky, Magloire Pakouzou, Boureima Dianda, Moctar Ousmane, Sié Kam, Dieudonné J Bathiebo. Air heating in a steady hemispherical concentrating system for various applications. International Journal of Current Research. 2018;10(2):65449-65454.
24. Ky TSM, Ouedraogo S, Ouedraogo A, Dianda B, Ousmane M, Bathiebo DJ. Novel convection process: experimental study of a solar chimney with its collector made of hemispherical concentrators. International Journal of Engineering Sciences & Research Technology. 2018;7(10):83-96.
25. Ky TSM, Dianda B, Ouedraogo E, Pakouzou BM, Kam S, Bathiebo DJ. Theoretical optical analysis of a spherical or a plat diopter on a hemispherical concentrator. Arabian Journal for Science and Engineering. 2019;44:6609–6620.
26. Vasylyev VP. Concentrator of radiant energy 'peresvet' and the manufacturing method. USSR Patent. 1981;SU1023270.
27. Mouzouris M, Roberts LW, Brooks M. Thermal performance of a high flux solar concentrating system. RED Journal of the South African Institute of Mechanical Engineering. 2011;27:10-22.
28. Cheng Zheng, Qiyuan Li, Gary Rosengarten, Evatt Hawkes, Robert A Taylor. A new optical concentrator design and analysis for rooftop solar applications; 2015.
29. Ky TSM, Bathiebo DJ. Capteur solaire fixe a production en température élevée. OAPI patent N°16893, BOPI N°02BR. 2015;23-24.

Peer-review history:
The peer review history for this paper can be accessed here:
http://www.sdiarticle4.com/review-history/66543